Comb-Shaped Supramolecules Based on Protonated Polyaniline and Their Self-Organization into Nanoscale Structures: Polyaniline Sulfonates/Zinc Sulfonates

7 AUTHORS, INCLUDING:

Manu Lahtinen
University of Jyväskylä
147 PUBLICATIONS   1,513 CITATIONS

Ritva Serimaa
University of Helsinki
236 PUBLICATIONS   5,504 CITATIONS

Kari Rissanen
University of Jyväskylä
668 PUBLICATIONS   10,809 CITATIONS

Comb-Shaped Supramolecules Based on Protonated Polyaniline and Their Self-Organization into Nanoscale Structures: Polyaniline Sulfonates/Zinc Sulfonates

Juha Hartikainen,[†] Manu Lahtinen,[§] Mika Torkkeli,[‡] Ritva Serimaa,[‡] Jussi Valkonen,[§] Kari Rissanen,*,[§] and Olli Ikkala*,[†]

Department of Engineering Physics and Mathematics, Helsinki University of Technology, P.O. Box 2200, FIN-02015 HUT, Espoo, Finland; Department of Physical Sciences, University of Helsinki, P.O. Box 64, FIN-00014, Helsinki, Finland; and Department of Chemistry, University of Jyväskylä, P.O. Box 35, FIN-40351, Jyväskylä, Finland

Received February 5, 2001; Revised Manuscript Received July 23, 2001

ABSTRACT: A concept is demonstrated for comb-shaped supramolecules based on dodecylbenzenesulfonic acid-doped polyaniline, i.e., $PANI(DBSA)_{0.5}$, by complexation with zinc dodecylbenzenesulfonate, $Zn(DBS)_2$. Model studies using related protonated single crystalline bipyridine oligomers suggest that $Zn(DBS)_2$ molecules are bonded by Zn^{2+}- and water-mediated hydrogen bonds to the sulfonates of $PANI(DBSA)_{0.5}$. The comb-shaped supramolecules, denoted as $PANI(DBSA)_{0.5}[Zn(DBS)_2]_x$ with $x = 0.25$, 0.5, 0.75, 1.0, and 1.5, self-organize as lamellar structures due to the repulsion between the alkyl chains and the polar moieties leading to plasticized materials. So far, the conductivity levels are low, i.e., in the range 10^{-7} S/cm, potentially requiring optimization of the lengths and the amounts of side groups. The concept allows generalization to complex functional groups along sulfonic acid protonated polyaniline chains.

Introduction

Supramolecules are well-defined structural entities that are formed due to specific intermolecular interactions, like *receptor and substrate*.[1,2] They can, in turn, assemble[3] or self-organize[4,5] (if they contain competing attractive and repulsive moieties) to allow hierarchies of nanoscale structures and can thus allow functional "molecule based materials".[6]

For supramolecules involving oligomers, there are numerous reports describing coordination,[1,2,7] combination of π-stacking with hydrogen bonds (see, e.g., ref 8), and hydrogen bonds (e.g., to render liquid crystals[9] or chainlike entities[1,10,11]). If polymeric components are involved, the comb-shaped architecture is known to render liquid crystallinity,[12−15] if shape-persistent groups are connected, or block copolymer-like[16,17] self-organization, if repulsive side chains are connected to the backbone using ionic interaction,[18] coordination,[19] or hydrogen bonding.[5,20] In the case of rigid conjugated polymers, improved solubility and self-organization can be achieved by covalently bonding flexible side chains to the backbone, leading to so-called hairy rods,[21,22] which are a special case of comb-shaped polymers or block copolymers. The corresponding *comb-shaped supramolecules*, where the side chains are physically bonded amphiphiles, are not straightforward to construct as the rigid backbones easily tend to macroscopically phase separate from the amphiphiles unless the attractive physical bonds are particularly strong. Proton transfer has been used to complex polyaniline (PANI) with dodecylbenzenesulfonic acid (DBSA),[23−25] dinonylnaphthalenesulfonic acid,[23,26] sulfophthalic acid alkyl esters,[27] camphorsulfonic acid (CSA),[23,28] or to complex polyquinoline[29] or poly(*p*-pyridine)[30] with DBSA. More complicated combinations of proton transfer and hydro-gen bonding to allow self-organization in conjugated polymers has also been described.[25,30−32] Finally, PANI−emeraldine base (PANI−EB) has been complexed using zinc dodecylbenzenesulfonate to allow self-organization, probably due to coordination between the iminic nitrogens and Zn^{2+} cations.[33]

PANI−EB can be doped for conductivity using strong acids.[34,35] PANI, whose iminic nitrogens are fully protonated using DBSA, i.e., $PANI(DBSA)_{0.5}$, is a crystalline solid.[24] It does not melt, and it is poorly soluble except in a few hydrogen bonding solvents like hexafluoro-2-propanol,[36] resorcinol,[37] or strong acids, such as formic acid. We posed the question as to whether we can connect a more dense set of alkyl side groups along the chain to further plasticize the polymer. Hydrogen bonding of additional DBSA molecules[25] to the aminic nitrogen would render excessive acidity. In this work, zinc dodecylbenzenesulfonate, i.e., $Zn(DBS)_2$, was used, the hypothesis being that $Zn(DBS)_2$ would coordinate to the aminic nitrogens of $PANI(DBSA)_{0.5}$. However, we will show that the complexation takes place, but in the bonding the crystalline water plays a role, probably to hydrogen bond zinc sulfonate to the sulfonates of $PANI(DBSA)_{0.5}$. In this respect, model studies using oligomeric bipyridine were essential.

Experimental Section

Materials. PANI−EB was supplied by Panipol Ltd. (Finland) and its molecular weight was $M_n = 16\,500$, as measured with GPC. 4,4′-Bipyridine (4,4′-Bpy) and racemic camphor sulfonic acid (CSA) were of 98% purity and supplied by Aldrich. ZnO was provided by Merck (purity 99%). Dodecylbenzenesulfonic acid (DBSA) was of purity 90% (Tokyo Kasei) and the main remaining impurity consisted of different chain lengths and branches: $(C_nH_{2n+1})(C_mH_{2m+1})CH-Ph-SO_3H$, with $n + m + 1 = 10...14$.
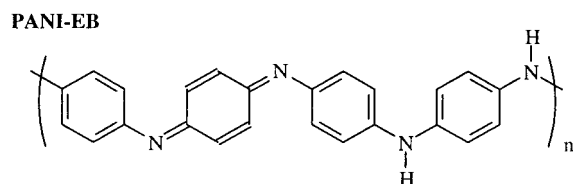
Sample Preparation. PANI−EB was dried at 40 °C in a vacuum (0.01 mbar) for 24 h. Its iminic nitrogens were nominally fully protonated, i.e., 0.5 mol of DBSA vs 1.0 mol of PANI−EB PhN repeat units. PANI−EB was added in formic

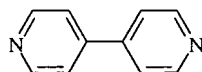[†] Helsinki University of Technology.
[‡] University of Helsinki.
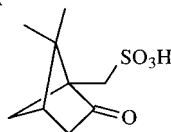[§] University of Jyväskylä.

Scheme 1

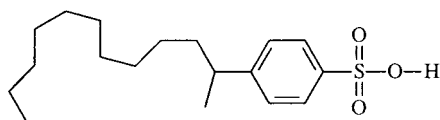**PANI-EB**

Scheme 2

4,4′-Bpy
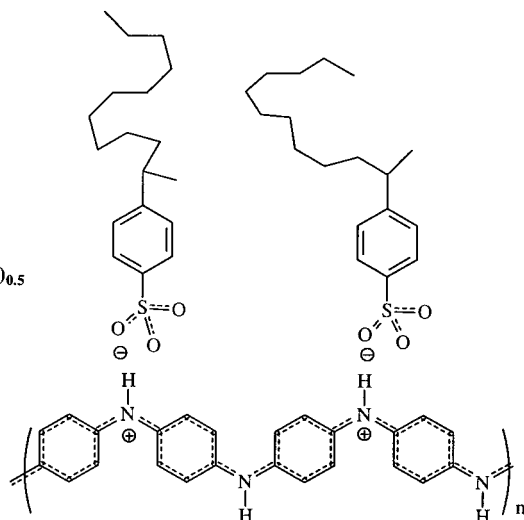

Scheme 3

CSA


Scheme 4

DBSA

Scheme 5

PANI(DBSA)₀.₅

acid (concentration of 1 wt %) and magnetically stirred 24 h which rendered a clear solution with no particles at the resolution of optical microscope. Next DBSA was added and mixing was continued for another 24 h, followed by formic acid evaporation on a hot stage at 50 °C, and the product was dried in a vacuum (0.01 mbar) at 40 °C for 24 h. The resulting material is denoted as PANI(DBSA)$_{0.5}$; see Scheme 5. That DBSA is able to protonate PANI is well-known from the literature.[23,24]

Zinc dodecylbenzenesulfonate Zn(DBS)$_2$ was synthesized in analysis grade ethanol from DBSA and ZnO according to

$$ZnO + 2DBSA \rightarrow Zn(DBS)_2 + H_2O$$
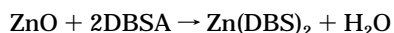
The product was recrystallized three times from acetone by adding distilled water dropwise. The FTIR spectra (Figure 1) suggest that Zn(DBS)$_2$ is formed as there is no unreacted
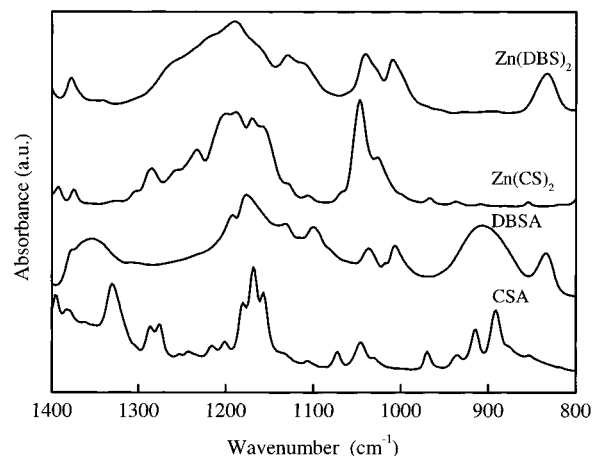

Figure 1. FTIR spectra of CSA, DBSA, Zn(CS)$_2$, and Zn-(DBS)$_2$ in the 1400−800 cm^{-1} region.

DBSA left because the sulfonic acid peak near 900 cm^{-1} is suppressed whereas the absorption for the ca. 1200 cm^{-1} band is increased due to sulfonate formation.

It turned out particularly difficult to find a solvent to prepare the complexes PANI(DBSA)$_{0.5}$[Zn(DBS)$_2$]$_x$. For example, hexafluoro-2-propanol or *m*-cresol were not common solvents for PANI(DBSA)$_{0.5}$ and Zn(DBS)$_2$. As inspired by our previous work,[37] we used resorcinol as a solvent, which unfortunately requires elevated temperatures due to its crystallinity (T_m = 102 °C). First, PANI(DBSA)$_{0.5}$ and Zn(DBS)$_2$ were ground together using mortar and pestle at the ratios 0.25, 0.50, 0.75, 1.00, and 1.50 mol/mol. Next, the ground mixtures were added to hot resorcinol (190 °C) and mixed with magnetic stirrer for 3 min under a nitrogen flux to reduce degradation. In all mixtures, the concentration of PANI-(DBSA)$_{0.5}$ was fixed at 1 wt %. To remove the solid solvent resorcinol, the samples were next inserted in a vacuum oven at 60 °C (0.1 mbar) for several days and finally at 80 °C (10^{-3} mbar) for 12 h. That most of the resorcinol could be removed under these conditions was monitored based on the weight losses, but we do not expect complete removal. This is not unexpected as there seems to be considerable solvent residuals also using other strongly bonded solvents even if they are liquids, e.g., *m*-cresol solvent in the case of PANI(CSA)$_{0.5}$ solvent casting.[38] In this work, the samples are denoted as PANI(DBSA)$_{0.5}$[Zn(DBS)$_2$]$_x$ according to their nominal compositions. We finally point out that, so far, we have not identified any liquidlike solvent that could be used to prepare the complexes.

To obtain more detailed information on the intermolecular interactions based on Zn^{2+}, sulfonates, and hydration water, we prepared additional oligomeric samples which were allowed to grow single crystals. Such materials can be helpful to learn about the associations although the actual structures can be different. Therefore, pyridine groups, which have much been used in supramolecular chemistry,[1,2] are useful, as they can be protonated, like the iminic nitrogens of PANI. 4,4′-Bipyridine (4,4′-Bpy) was selected, both of its pyridine nitrogens were protonated with DBSA, and (4,4′-Bpy)(DBSA)$_2$ was complexed with two Zn(DBS)$_2$ molecules. Such a stoichiometry is justified, as we later point out, because the Zn^{2+} cations become complexed to the sulfonates of the protonating acids. The (4,4′-Bpy)(DBSA)$_2$[Zn(DBS)$_2$]$_2$ complexes, however, did not easily allow growing of single crystals, probably due to the long plasticizing alkyl chains. As inspired by the role of CSA in the context of PANI, we made the corresponding complexes using CSA: A stoichiometric complex of 4,4′-Bpy and CSA at their ratio 1.0/2.0 mol/mol, i.e., 4,4′-Bpy(CSA)$_2$, was prepared from 5 wt % methanol solution, evaporated, and dried at 40 °C in a vacuum; see Scheme 6. Zinc camphorsulfonate Zn(CS)$_2$ was prepared from ZnO and CSA in ethanol, and the product was purified by recrystallizing once from acetone. As in the case of Zn(DBS)$_2$, Figure 1 also suggests that the salt Zn(CS)$_2$ is

Scheme 6
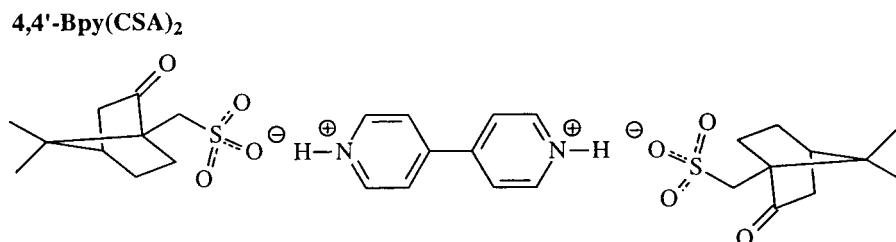
4,4'-Bpy(CSA)$_2$

formed. The expected stoichiometric complex where there is one $Zn(CS)_2$ molecule corresponding to each camphorsulfonate anion, i.e., 4,4′-Bpy(CSA)$_2$[Zn(CS)$_2$]$_2$, was prepared from methanol solution. After mixing for 4 h with magnetic stirrer, the solvent was evaporated and the sample dried in a vacuum oven at 40 °C.

Optical Microscopy. A Nikon Optiphot 66 microscope was used to study the homogeneity of the solutions and films at a crude level.

FT-IR Spectroscopy. 4,4′-Bpy samples were analyzed from films cast on potassium bromide pellets using a Nicolet Magna IR 750 FT-IR spectrometer (the minimum number of scans 64). PANI samples were analyzed from samples ground within potassium bromide using mortar and then pressed to pellets.

UV–Vis Spectroscopy. A Hitachi U2000 spectrophotometer was used. The samples were pressed between two quartz glasses at 190 °C.

Small-Angle X-ray Scattering. See previous reports for details.[39]

Wide Angle X-ray Scattering. The X-ray powder diffraction studies of 4,4′-Bpy(CSA)$_2$[Zn(CS)$_2$]$_2$ samples were carried out with a Nonius PSD 120. The measurements were performed with Cu Kα_1 radiation ($\lambda = 1.541$ Å) selected by a primary beam germanium monochromator ($d = 3.266$ Å). Reflection geometry with the sample surface at fixed angle of 8° to the incident beam was used. The diffraction patterns were measured with an Inel CPS120 curved position sensitive detector (PSD) for 2θ in the range 8–120°. Recording time was 10 min.

Dried 4,4′-Bpy samples were measured using an Anton Paar XRK in situ high-temperature reaction chamber under dried N$_2$ gas (purity 99.9996%). For humid 4,4′-Bpy samples, it sufficed to let the samples absorb atmospheric humidity for ca. 3 h at 21 °C.

Single-Crystal X-ray Diffraction. Nonius Kappa CCD area-detector diffractometer using graphite monochromatized Mo Kα radiation ($\lambda = 0.710\ 73$ Å) was used. Lattice parameters were determined from 10 images recorded with 1° φ scans and subsequently refined on all data. The data collections were performed using φ and ω scans with or 2° steps with an exposure time of 30 s per frame and the crystal-to-detector distance fixed to 35 mm. The data were processed using DENZO-SMN v0.93.0.[40]

The structure was solved by direct methods and refined on F^2 using SHELXL-97.[41] The hydrogen atoms for 4,4′-Bpy were calculated to their idealized positions with isotropic temperature factors (1.2 the carbon temperature factor) and refined as riding atoms. The H atoms of the water molecules coordinated to zinc were found in the difference Fourier map and were refined with constraints (fixed O–H distance 1.0 Å) to keep them chemically reasonable. The bicyclic camphorsulfotate moieties were disordered and the electron density of them was modeled using only isotopically refined C atoms (O− or H-atoms could not be located). The resolved atoms were refined anisotropically giving a reasonable R factor.

Results and Discussion

First we will investigate whether the complexation between PANI(DBSA)$_{0.5}$ and Zn(DBS)$_2$ takes place. Optical microscopy shows homogeneously green and transparent mixtures of PANI(DBSA)$_{0.5}$, Zn(DBS)$_2$ and
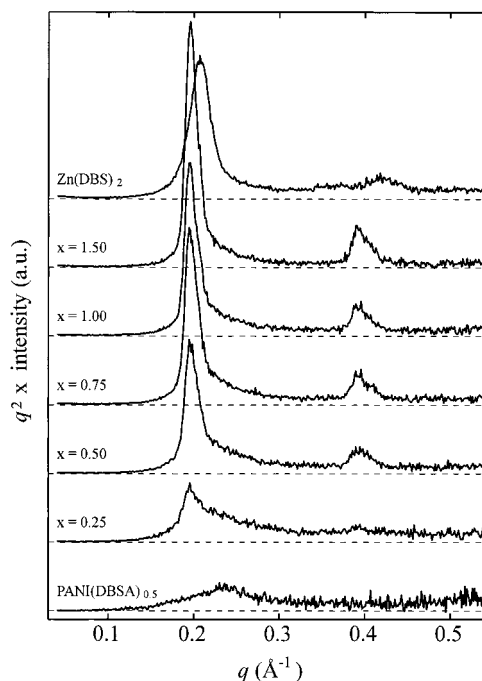
Figure 2. SAXS intensity curves of PANI(DBSA)$_{0.5}$[Zn-(DBS)$_2$]$_x$ with $x = 0.25$, 0.50, 0.75, 1.00, and 1.50, as well as the intensity curves of neat Zn(DBS)$_2$ and PANI(DBSA)$_{0.5}$. The magnitude of the scattering vector is given by $q = (4\pi/\lambda) \sin(\theta)$ where 2θ is the scattering angle.

**Table 1. Suggested Correspondence between the PANI and 4,4′-Bpy Complexes**

|	PANI complex	4,4′-Bpy complex
base form	PANI	4,4′-Bpy
fully protonated salt form	PANI(DBSA)$_{0.5}$	4,4′-Bpy(CSA)$_2$
one zinc sulfonate for each protonating sulfonic acid	PANI(DBSA)$_{0.5}$-[Zn(DBS)$_2$]$_{0.50}$	4,4′-Bpy(CSA)$_2$-[Zn(CS)$_2$]$_2$

resorcinol at 190 °C for the present compositions. This suggests that at this resolution resorcinol is a common solvent for PANI(DBSA)$_{0.5}$ and Zn(DBS)$_2$ at the high temperatures. Even after removal of resorcinol by vacuum-drying, optical microscopy shows a homogeneous structure, suggesting that PANI(DBSA)$_{0.5}$ dissolves in Zn(DBS)$_2$.

X-ray scattering and FT-IR render more definite conclusions on the complexation. SAXS results of PANI-(DBSA)$_{0.5}$[Zn(DBS)$_2$]$_x$ are depicted in Figure 2. The magnitudes of the scattering vector at the first intensity maxima q^* and the corresponding long periods are presented in Table 2. Zn(DBS)$_2$ is lamellar mesomorphic,[19,42,43] which is observed also in the present case as there is a faint second-order peak at $2q^*$. The long period is 30.4 Å. The solid and hard PANI(DBSA)$_{0.5}$ shows only a broad maximum at $q \cong 0.23$ Å^{-1} in the SAXS regime. Interestingly, PANI(DBSA)$_{0.5}$[Zn(DBS)$_2$]$_x$ show lamellar mesomorphic structures: In the case of
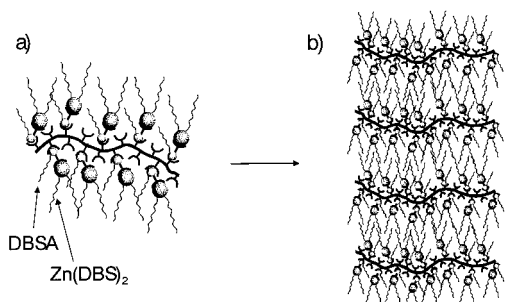
Figure 3. Schematic illustrations: (a) the comb-shaped supramolecule based on complexation between PANI(DBSA)$_{0.5}$ and Zn(DBS)$_2$; (b) the lamellar self-organization of PANI-(DBSA)$_{0.5}$[Zn(DBS)$_2$]$_{0.50}$.
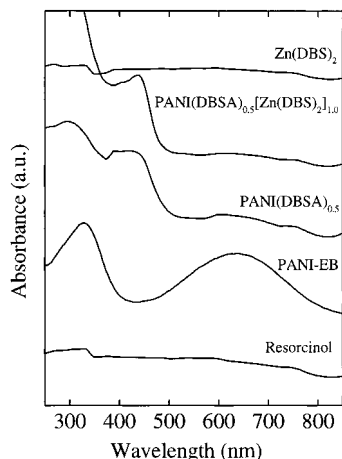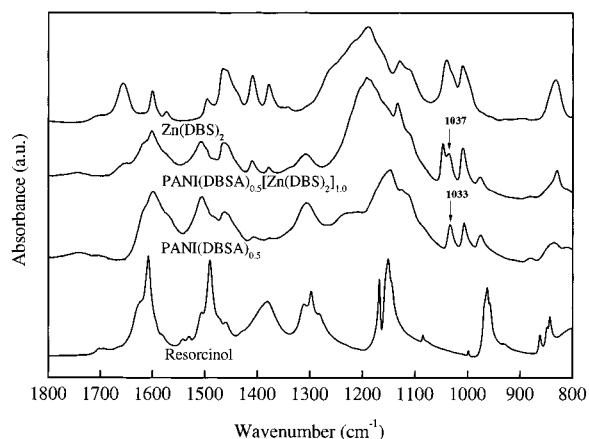

Figure 4. UV–vis spectra of PANI-EB, PANI(DBSA)$_{0.5}$, PANI(DBSA)$_{0.5}$[Zn(DBS)$_2$]$_{1.0}$, Zn(DBS)$_2$, and resorcinol.

Table 2. SAXS Data for PANI(DBSA)$_{0.5}$[Zn(DBS)$_2$]$_x$ Complexes

PANI(DBSA)$_{0.5}$-[Zn(DBS)$_2$]$_x$	q^* (Å^{-1})	$L_p = 2\pi/q^*$ (Å)
PANI(DBSA)$_{0.5}$	0.230	27.3
$x = 0.25$	0.196	32.1
0.50	0.194	32.4
0.75	0.194	32.4
1.00	0.194	32.4
1.50	0.196	32.1
Zn(DBS)$_2$	0.207	30.4

$x = 0.25$, scattering peaks are observed at $q^* = 0.196$ Å^{-1} and at $2q^*$, suggesting lamellar self-organization with a layer thickness of 32.1 Å. The peaks become more distinct as the mole fraction of Zn(DBS)$_2$ is increased and relatively narrow peaks are observed for $x = 1.50$. In PANI(DBSA)$_{0.5}$[Zn(DBS)$_2$]$_x$, the increased long period in comparison to pure Zn(DBS)$_2$ is in agreement with the hypothesis that the complexes are formed and that the increased long period is due to thicker polar layers. Figure 3 shows schematically the proposed lamellar self-organization of PANI(DBSA)$_{0.5}$[Zn(DBS)$_2$]$_x$ consisting of the alternating alkyl layers (dodecyl tails of Zn(DBS)$_2$ and DBSA) and polar layers (containing also the PANI chains).

As the samples are prepared at relatively high temperature (190 °C), it was studied whether degradation might take place. PANI doped with toluenesulfonic acid is stable up to ca. 300 °C,[44] suggesting that aromatic sulfonic acids can allow high thermal stability. Figure 4 shows UV–vis spectra after the resorcinol treatment where the typical absorption band of acid-doped PANI


Figure 5. FTIR spectra of PANI(DBSA)$_{0.5}$, PANI(DBSA)$_{0.5}$-[Zn(DBS)$_2$]$_{1.0}$, Zn(DBS)$_2$, and resorcinol in the 1800–800 cm^{-1} region.

at ca. 450 nm is observed instead of the characteristic band of the undoped form at ca. 600 nm (see e.g., refs 45 and 46). On the basis of this observation, in combination with the aromatic nature of the dopant and short mixing time under N$_2$ atmosphere, we did not expect major degradation.

Figure 5 depicts the FTIR spectrum of PANI(DBSA)$_{0.5}$-[Zn(DBS)$_2$]$_{1.0}$, as well as those of PANI(DBSA)$_{0.5}$, Zn-(DBS)$_2$, and resorcinol. PANI(DBSA)$_{0.5}$ and PANI-(DBSA)$_{0.5}$[Zn(DBS)$_2$]$_{1.0}$ have been prepared from the resorcinol solvent, but the spectrum of Zn(DBS)$_2$ is measured from the starting material without resorcinol treatment as a reference. Characteristic absorptions of resorcinol at ca. 3300 cm^{-1} (not shown), as well as near 1600 and 1500 cm^{-1} can be observed also in the resorcinol-treated PANI samples, which indicates that there is still some residual resorcinol after the extended drying procedure. Thus, as the aminic (ca. 1600 cm^{-1}) and iminic (ca. 1500 cm^{-1}) absorption bands of PANI overlap with the bands of resorcinol, and minor changes at these characteristic bands cannot unambiguously be detected using FTIR. However, small changes can be observed near 1030 cm^{-1} which can be assigned to the SO stretching bands: PANI(DBSA)$_{0.5}$ has an absorption at 1033 cm^{-1}, and in PANI(DBSA)$_{0.5}$[Zn(DBS)$_2$]$_{1.0}$ a shoulder at a ca. 1037 cm^{-1} is observed, which we cannot assign at present. However, its overall position suggests that the sulfonates of PANI(DBSA)$_{0.5}$ play a role in the complexation of Zn(DBS)$_2$, potentially mediated by Zn^{2+}. Note that PANI(DBSA)$_{0.5}$ has additional aminic groups which could be considered as potential coordination sites for Zn^{2+} due to their electron pairs. However, upon sulfonic acid doping, there is positive charge transferred to PANI, and therefore, the tendency to coordination to the PANI amines might be suppressed.

Single crystalline samples were next pursued to allow assignment of atomic locii using WAXS. We investigated oligomeric model compounds based on 4,4′-bipyridine (4,4′-Bpy) based on the following logic: First, the two nitrogens of 4,4′-Bpy can be protonated, coordinated, or hydrogen bonded[39] like the iminic nitrogens of the emeraldine base form of PANI. Therefore, the fully protonated 4,4′-Bpy(CSA)$_2$ corresponds to the fully protonated PANI(CSA)$_{0.5}$. Second, 4,4′-Bpy has smaller molecular weight than the PANI−EB oligomers (which consist of at least four aromatic rings) which we expected to promote facile growth of single crystals. For
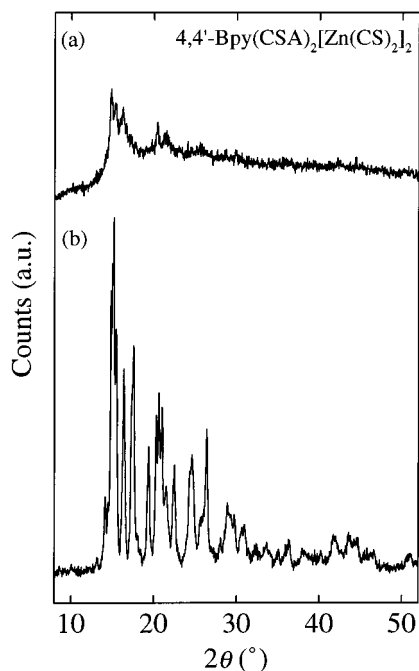
Figure 6. (a) Powder WAXS intensity curves of the oligomeric model compound 4,4′-Bpy(CSA)$_2$[Zn(CS)$_2$]$_2$. The sample is dried at 60 °C in a vacuum and measured under nitrogen flow. (b) WAXS intensity curve of the same material after absorbing atmospheric humidity for 3 h.

the same reason, camphorsulfonic acid was chosen as a counterion instead of DBSA, i.e., to promote crystallinity. Therefore, an underlying hypothesis is that there exists an analogy between the PANI and 4,4′-Bpy-complexes, see Table 1, which can be used to learn on the complexation of Zn^{2+}. Note that the overall structures may be in detail different and the analogy must used in a great care.

Before going to the WAXS data, it becomes relevant to consider the role of water: The materials consisting of sulfonates are very hygroscopic and we do not expect that the presently used relatively mild drying conditions result in a complete removal of absorbed water. On the other hand, the shifts in the SO stretching bands are small (Figure 5) which does not easily suggest coordination between Zn^{2+} and sulfonate group. Some other mechanisms might take place instead, where the almost inevitably absorbed water could play a role.

First, WAXS was performed on powdered 4,4′-Bpy-(CSA)$_2$[Zn(CS)$_2$]$_2$ samples. Dried samples under N$_2$ flow showed relatively poor crystallization whereas samples that were allowed to absorb atmospheric humidity show sharp WAXS peaks; see Figure 6. This shows the importance of water in the structures. To resolve the role of water, single crystals of 4,4′-Bpy(CSA)$_2$[Zn(CS)$_2$]$_2$ were grown upon slow methanol evaporation under atmospheric conditions. The crystal data measured at the temperature of −100 °C is shown in Table 3 as well as in Figures 7 and 8. The structure consists of four types of moieties: 4,4′-bipyridinium cations, camphorsulfonate anions, Zn^{2+}, and water molecules coordinated to Zn^{2+}. Zn^{2+} is surrounded by six water molecules in the first hydration sphere due to charge/dipole interaction; see also Figure 8. The water molecules, in turn, mediate the fully saturated hydrogen bond system to the electronegative oxygens of the sulfonate anions with the distance being between 2.6 and 2.8 Å. Two of the sulfonate anions act as tridentate hydrogen bond bridges
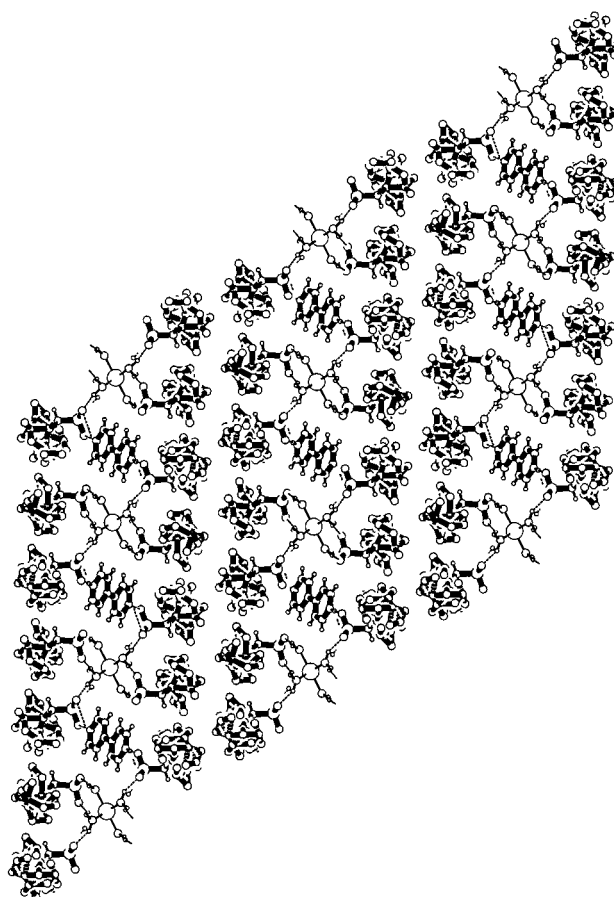

Figure 7. Illustration of the crystal structure of hexahydrated 4,4′-Bpy(CSA)$_2$[Zn(CS)$_2$]$_2$ resolved from the single-crystal WAXS results presented in Table 3.

Table 3. Crystal Data and Structure Refinement for 4,4′-Bpy(CSA)$_2$[Zn(CS)$_2$]$_2$·6H$_2$O

empirical formula	C$_{50}$H$_{82}$N$_2$O$_{22}$S$_4$Zn
X-ray formula	C$_{81.5}$H$_{30}$N$_2$O$_{18}$S$_4$Zn
fw	1518.68
temp	173(2) K
wavelength	0.71073 Å
cryst syst	monoclinic
space group	$C2/c$
unit cell dimens	$a = 42.6198(10)$ Å; $\alpha = 90°$
	$b = 6.88850(10)$ Å; $\beta = 125.5480(10)°$
	$c = 24.7704(10)$ Å; $\gamma = 90°$
vol	5916.9(3) Å^3
Z	4
density (calcd from X-ray formula)	1.705 Mg/m^3
abs coeff	0.647 mm^{-1}
F(000)	3084
cryst size	0.2 × 0.3 × 0.3 mm^3
θ range	3.01 to 25.67°.
index ranges	$-51 < h < 51$
	$-8 < k < 8$
	$-30 < l < 30$
no. of reflcns	17 781
no of indep reflcns	5294 [R(int) = 0.0628]
completeness to $\theta = 25.67°$	94.2%
refinement method	full-matrix least-squares on F^2
data/restraints/params	5294/6/390
goodness-of-fit on F^2	1.081
final R indices [$I > 2\sigma(I)$]	R1 = 0.1049, wR2 = 0.2670
R indices (all data)	R1 = 0.1456, wR2 = 0.2979
extinction coeff	0.0029(4)
largest diff peak and hole	+0.774 and −0.890 e·Å^{-3}

connecting two adjacent hexahydrated Zn^{2+} ions, thus creating a hydrogen-bonded [···Zn^{2+}(H$_2$O)$_6$···(CS)$_2$···
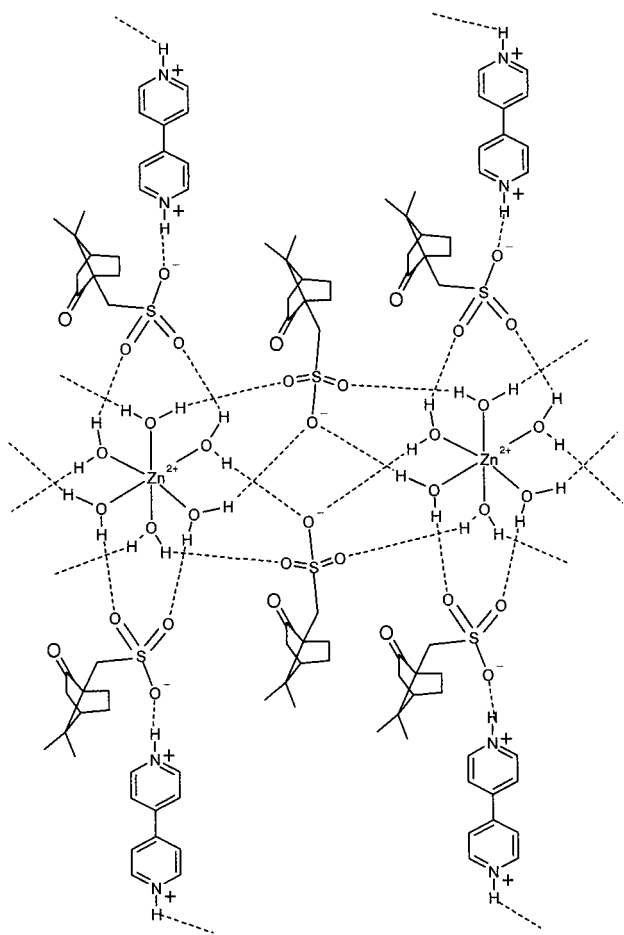
Figure 8. Schematic illustration of 4,4'-Bpy(CSA)$_2$[Zn(CS)$_2$]$_2$ based on the single-crystal WAXS analysis showing geometry of the hydrogen bonds. We suggest that analogous hydrogen bonds also connect PANI(DBSA)$_{0.5}$ and Zn(DBS)$_2$.

Zn^{2+}(H$_2$O)$_6$···(CS)$_2$···] 1-dimensional array along the Y axis. The two remaining sulfonate anions are hydrogen bonded to the remaining H atoms of the water molecules by two of the sulfonate oxygens. The last sulfonate oxygen acts as a hydrogen bond donor to the protonated 4,4'-Bpy molecule, which in turn connects the adjacent 1-dimensional arrays into a layer perpendicular to the Y-axis. The layers, in turn, are held together by hydrophobic interactions between the nonpolar camphor moieties (see Figure 7). Therefore, the water molecules play a central role in the physical bonding between Zn(CS)$_2$ and 4,4'-Bpy(CSA)$_2$. The obvious next question concerns the physical bonds upon drying. At present, we are not able to answer such a question as the structure is poor (see Figure 6a). However, it seems to us probable that there may always be some residual water to mediate the bond between 4,4'-Bpy and Zn(CS)$_2$.

Our hypothesis, which however remains unproven so far, is that even in PANI(DBSA)$_{0.5}$[Zn(DBS)$_2$]$_{0.5}$ a similar mechanism might take place to bond Zn(DBS)$_2$ to the sulfonate groups of PANI(DBSA)$_{0.5}$ based on water-mediated hydrogen bonds. Furthermore, we suggest that additional Zn(DBS)$_2$ molecules may, in turn, be hydrogen bonded to the already bonded sulfonates similarly, based on hydrogen bonds mediated by additional water molecules. Accordingly, additional Zn(DBS)$_2$ might be "plugged" along PANI(DBSA)$_{0.5}$ to tailor the level of plasticization.

Finally, another point of view can be taken to link the present considerations to ionomer blends. Ionomers are polymers containing relatively dilute molar fraction of ionic groups, causing microphase separation to charged multiplets.[47,48] Physical interactions due to ions can be used to compatibilize blends[49] where, e.g., zinc sulfonate-containing polymers become compatibilized with amine-[50] or amide-containing[51,52] polymers. The specific interaction can form due to coordination where the nitrogen-containing group replaces hydration water. Accordingly, another point of view to consider the present work is that the blend consisting of DBSA-doped PANI and additional alkyl chains is "compatibilized" by the sulfonate groups of the dopant DBSA and zinc sulfonate groups of Zn(DBS)$_2$ to provide lamellar microphase-separated domains. Note that for ionomer blends, rather severe conditions have been used when dehydrated samples are pursued, e.g., drying at 160 °C.[53] Extended drying at such temperatures could be detrimental for the present samples containing low molecular weight components. Therefore, the present samples are expected to contain some hydration water almost inevitably.

Finally, conductivities of PANI(DBSA)$_{0.5}$[Zn(DBS)$_2$]$_x$ are addressed. Preliminary measurements show that the conductivities are low, i.e., on the order of 10^{-7} S/cm as measured from pressed pellets. So far, the reason for this low conductivity remains open. One of the potential reasons is that by increasing the alkyl and other spacer groups between the chains, the conductivity may become reduced, as shown, e.g., in the case of different alkyl-benzenesulfonic acids[54] and dinonylnaphthalenesulfonic acid.[26] The conductivity will be considered in more detail in our future studies.

Concluding Remarks

We have discussed a concept to achieve comb-shaped supramolecules with alkyl "combs" based on sulfonic acid-doped polyaniline and their self-organization into nanoscale structures. In particular, we have shown by SAXS that PANI(DBSA)$_{0.5}$ can be complexed with Zn(DBS)$_2$ to form lamellar mesomorphic structures. To assign the mechanism of the complexation, we also discussed hydrated single crystalline stoichiometric oligomeric complexes between 4,4'-Bpy(CSA)$_2$ and Zn(CS)$_2$. The crystal structure of 4,4,'-Bpy(CSA)$_2$[Zn(CS)$_2$]$_2$ shows that water molecules of the hexahydrated Zn^{2+} form a complicated, yet defined, highly organized hydrogen bond network creating 1D arrays in the crystal lattice. An analogical hydration-induced bonding is suggested also between PANI(DBSA)$_{0.5}$ and Zn(DBS)$_2$. Such interactions are suggested to provide a general route to connect surface active groups along sulfonic acid-doped PANI where due to the aggregation tendency, the polymer rigidity, and internal hydrogen bonds, particularly strong attraction is required to achieve complexation. We believe that the concept is rather general and ultimately allows a method to tailor the processability of sulfonic acid-doped PANI.

References and Notes

(1) Lehn, J.-M. *Supramolecular Chemistry*; VCH: Weinheim, Germany, 1995.

(2) Vögtle, F. *Supramolecular Chemistry*; John Wiley & Sons: Chichester, 1993.

(3) Fyfe, M. C. T.; Stoddart, J. F. *Acc. Chem. Res.* **1997**, *30*, 393.

(4) Stupp, S. I.; LeBonheur, V.; Walker, K.; Li, L. S.; Huggins, K. E.; Keser, M.; Amstutz, A. *Science* **1997**, *276*, 384.

(5) Ruokolainen, J.; Mäkinen, R.; Torkkeli, M.; Serimaa, R.; Mäkelä, T.; ten Brinke, G.; Ikkala, O. *Science* **1998**, *280*, 557.

(6) Alivisatos, A. P.; Barbara, P. F.; Castleman, A. W.; Chang, J.; Dixon, D. A.; Klein, M. L.; McLendon, G. L.; Miller, J. S.; Ratner, M. A.; Rossky, P. J.; Stupp, S. I.; Thompson, M. E. *Adv. Mater.* **1998**, *10*, 1297.

(7) *Transition Metals in Supramolecular Chemistry*; Sauvage, J.-P.; Ed.; John Wiley & Sons: Chichester, England, 1999.

(8) Rebek, J. *Top. Curr. Chem.* **1988**, *149*, 189.

(9) Brienne, M.-J.; Gabard, J.; Lehn, J.-M.; Stibor, I. *J. Chem. Soc., Chem. Commun.* **1989**, *24*, 1868.

(10) Pfaadt, M.; Moessner, G.; Pressner, D.; Valiyaveettil, S.; Boeffel, C.; Müllen, K.; Spiess, H. W. *J. Mater. Chem.* **1995**, *5*, 2195.

(11) Sijbesma, R. P.; Beijer, F. H.; Brunsveld, L.; Folmer, B. J. B.; Hirschberg, J. H. K. K.; Lange, R. F. M.; Lowe, J. K. L.; Meijer, E. W. *Science* **1997**, *278*, 1601.

(12) Kato, T.; Fréchet, J. M. J. *Macromolecules* **1989**, *22*, 3818.

(13) Kato, T.; Nakano, M.; Moteki, T.; Uryu, T.; Ujiie, S. *Macromolecules* **1995**, *28*, 8875.

(14) Brandys, F. A.; Bazuin, C. G. *Chem. Mater.* **1996**, *8*, 83.

(15) *Mechanical and Thermophysical Properties of Polymer Liquid Crystals*; 1st ed.; Brostow, W., Ed.; Chapman & Hall: London, 1998.

(16) Hamley, I. W. *The physics of block copolymers*; Oxford University Press: Oxford, England, 1998.

(17) Bates, F. S.; Fredrickson, G. H. *Annu. Rev. Phys. Chem.* **1990**, *41*, 525.

(18) Antonietti, M.; Conrad, J.; Thünemann, A. *Macromolecules* **1994**, *27*, 6007.

(19) Ruokolainen, J.; Tanner, J.; ten Brinke, G.; Ikkala, O.; Torkkeli, M.; Serimaa, R. *Macromolecules* **1995**, *28*, 7779.

(20) Ruokolainen, J.; Tanner, J.; Ikkala, O.; ten Brinke, G.; Thomas, E. L. *Macromolecules* **1998**, *31*, 3532.

(21) Ballauff, M. *Angew. Chem., Int. Ed. Engl.* **1989**, *28*, 253.

(22) Wegner, G. *Thin Solid Films* **1992**, *216*, 105.

(23) Cao, Y.; Smith, P.; Heeger, A. J. *Synth. Met.* **1992**, *48*, 91.

(24) Yang, C. Y.; Smith, P.; Heeger, A. J.; Cao, Y.; Österholm, J.-E. *Polymer* **1994**, *35*, 1142.

(25) Zheng, W.-Y.; Wang, R.-H.; Levon, K.; Rong, Z. Y.; Taka, T.; Pan, W. *Makromol. Chem. Phys.* **1995**, *196*, 2443.

(26) Kinlen, P. J.; Liu, J.; Ding, Y.; Graham, C. R.; Remsen, E. E. *Macromolecules* **1998**, *31*, 1735.

(27) Kulszewicz-Bajer, I.; Zagórska, M.; Niziol, J.; Pron, A.; Luzny, W. *Synth. Met.* **2000**, *114*, 125.

(28) Cao, Y.; Smith, P.; Yang, C. *Synth. Met.* **1995**, *69*, 191.

(29) van der Sanden, M. C. M.; Yang, C. Y.; Smith, P.; Heeger, A. J. *Synth. Met.* **1996**, *78*, 47.

(30) Knaapila, M.; Ruokolainen, J.; Torkkeli, M.; Serimaa, R.; Horsburgh, L.; Monkman, A. P.; Bras, W.; ten Brinke, G.; Ikkala, O. *Synth. Met.* **2001**, *121*, 1257.

(31) Ikkala, O.; Knaapila, M.; Ruokolainen, J.; Torkkeli, M.; Serimaa, R.; Jokela, K.; Horsburgh, L.; Monkman, A. P.; ten Brinke, G. *Adv. Mater.* **1999**, *11*, 1206.

(32) Kosonen, H.; Ruokolainen, J.; Knaapila, M.; Torkkeli, M.; Jokela, K.; Serimaa, R.; ten Brinke, G.; Bras, W.; Monkman, A. P.; Ikkala, O. *Macromolecules* **2000**, *33*, 8671.

(33) Ruokolainen, J.; Eerikäinen, H.; Torkkeli, M.; Serimaa, R.; Jussila, M.; Ikkala, O. *Macromolecules,* **2000**, *33*, 9272.

(34) Doriomedoff, M.; Hautiere-Cristofini, F.; Surville, R. D.; Jozefowicz, M.; Yu, L.-T.; Buvet, R. *J. Chim. Phys. Physicochim. Biol.* **1971**, *68*, 1055.

(35) Chiang, J.-C.; MacDiarmid, A. G. *Synth. Met.* **1986**, *13*, 193.

(36) Hopkins, A. R.; Rasmussen, P. G.; Basheer, R. A. *Macromolecules* **1996**, *29*, 7838.

(37) Vikki, T.; Pietilä, L.-O.; Österholm, H.; Ahjopalo, L.; Takala, A.; Toivo, A.; Levon, K.; Passiniemi, P.; Ikkala, O. *Macromolecules* **1996**, *29*, 2945.

(38) MacDiarmid, A. G.; Epstein, A. J. *Synth. Met.* **1994**, *65*, 103.

(39) Ruokolainen, J.; Torkkeli, M.; Serimaa, R.; Vahvaselkä, S.; Saariaho, M.; ten Brinke, G.; Ikkala, O. *Macromolecules* **1996**, *29*, 6621.

(40) Otwinowski, Z.; Minor, W. In *Methods in Enzymology, Macromolecular Crystallography*; Carter, C. W. J., Sweet, R. M., Eds.; Academic Press: New York, 1997; Vol. A.

(41) Sheldrick, G. M. SHELXS-97, A Program Crystal Structure Refinement. University of Göttingen, Göttingen, Germany, 1997.

(42) Tezak, D.; Strajnar, F.; Milat, O.; Stubicar, M. *Prog. Colloid Polym. Sci.* **1984**, *69*, 100.

(43) Motamedi, F. *Liq. Cryst.* **1997**, *22*, 749.

(44) Jen, K.-Y.; Elsenbaumer, R. L. U.S. Patent 5,069,820, 1991.

(45) Stejskal, J.; Kratochvil, P.; Radhakrishnan, N. *Synth. Met.* **1993**, *61*, 225.

(46) Xia, Y.; Wiesinger, J. M.; MacDiarmid, A. G.; Epstein, A. J. *Chem. Mater.* **1995**, *7*, 443.

(47) Eisenberg, A.; Kim, J.-S. *Introduction to Ionomers*; Wiley: New York, 1998.

(48) Peiffer, D. G.; Weiss, R. A.; Lundberg, R. D. *J. Polym. Sci., Polym. Phys. Ed.* **1982**, *20*, 1503.

(49) Bazuin, C. G. In *Polymer Materials Encyclopedia*; Salamone, J. C., Ed.; CRC Press: Boca Raton, FL, 1996.

(50) Peiffer, D. G.; Duvdevani, I.; Agarwal, P. K.; Lundberg, R. D. *J. Polym. Sci., Polym. Lett. Ed.* **1986**, *24*, 581.

(51) Frunze, T. M.; Shleifman, R. B.; Kurashev, V. V.; Genin, Y. V.; Dubovik, I. I.; Slonismskii, G. L. *Polym. Sci. USSR* **1988**, *30*, 764.

(52) Lu, X.; Weiss, R. A. *Macromolecules* **1992**, *25*, 6185.

(53) Register, R. A.; Bell, T. *J. Polym. Sci., Polym. Phys. Ed.* **1992**, *30*, 569.

(54) Kobayashi, A.; Xu, X.; Ishikawa, H.; Satoh, M.; Hasegawa, E. *J. Appl. Phys.* **1992**, *72*, 5702.